

(Supplementary Information)

Luminescent iridium(III)-pyridyl based complexes: tumor inhibitory studies in 4T1 mammary carcinoma mice model

Natesan Sundarmurthy Karthikeyan¹, Shishu Kant Suman^{2*}, Prasad P. Phadnis^{3,4*}, Lalrinawma Zote^{3,5}, Chandan Kumar^{2,6} and Vasanthakumaran Sudarsan^{3,4}

¹Department of Chemistry, Easwari Engineering College, Chennai 600089, Tamil Nadu, India

²Radiopharmaceuticals Division, Bhabha Atomic Research Centre, Mumbai 400085, Maharashtra, India

³Chemistry Division, Bhabha Atomic Research Centre, Mumbai 400085, Maharashtra, India

⁴Chemical Sciences, Homi Bhabha National Institute, Mumbai 400094, Maharashtra, India

⁵Department of Chemistry, Mizoram University, Aizawl 796004, Mizoram, India

⁶Life Sciences, Homi Bhabha National Institute, Mumbai 400094, Maharashtra, India

***Correspondence:** Prasad P. Phadnis, Chemistry Division, Bhabha Atomic Research Centre, Trombay, Mumbai 400085, Maharashtra, India. phadnisp@barc.gov.in | Shishu Kant Suman, Radiopharmaceuticals Division, Bhabha Atomic Research Centre, Trombay, Mumbai 400085, Maharashtra, India. shishu@barc.gov.in

ORCID:

Natesan Sundarmurthy Karthikeyan (<https://orcid.org/0000-0002-1822-0883>)

Shishu Kant Suman (<https://orcid.org/0000-0002-8236-4750>)

Prasad P. Phadnis (<https://orcid.org/0000-0001-6423-631X>)

Lalrinawma Zote (<https://orcid.org/0000-0003-4179-4591>)

Chandan Kumar (<https://orcid.org/0000-0002-2214-9792>)

Vasanthakumaran Sudarsan (<https://orcid.org/0000-0003-4183-6560>)

Contents

No.	Description	Page no.
1	Synthesis of 4-phenyl-2-(thiophen-2-yl) quinoline (TPQ) ligand	S-2
2	Synthesis scheme of [(TPQ) ₂ Ir ₃] (1) complex & characterization	S-2
3	Synthesis scheme of [(TPQ) ₂ Ir(4-EO ₂ -pic)] (2) complex & characterization	S-5
4	Synthesis scheme of [(ppy) ₂ Ir(dfmpy)] (3) complex & characterization	S-8
5	Flow cytometry overlay histogram	S-10
6	Bar chart for internalization of [Ir(TPQ)₂(4-EO₂-pic)] (2)	S-11

1 Synthesis of 4-phenyl-2-(thiophen-2-yl) quinoline (TPQ) ligand

The ligand, 4-phenyl-2-(thiophen-2-yl) quinoline was synthesized using reported method with slight modification. 1-(thiophen-2-yl)ethanone (1 eq. 11.89 mmol), diphenyl phosphate (1 eq. 11.89 mmol), 2-aminobenzophenone (1 eq. 11.89 mmol) and *m*-cresol (25 mL) were added to a 100 mL round-bottomed flask and the mixture was refluxed for 12 h under a nitrogen atmosphere. After cooling the reaction mixture to room temperature, the solvent was evaporated *in vacuo*, and the resulting residue was poured into a 10% NaOH_{aq} solution and extracted with CH₂Cl₂ and dried over anhydrous NaSO₄. The resulting crude product was further purified by column chromatography with hexane and ethyl acetate (9:1 v/v) to afford the primary ligand as an amorphous white solid (2.65 g, 75%). The purified product was fully characterized by ¹H NMR and ¹³C{¹H} NMR. ¹H NMR (400 MHz, CDCl₃): δ 8.19-8.16 (d, 1H, Ar H), 8.06-8.05 (dd, 1H, Ar H), 7.90-7.86 (m, 2H, Ar H), 7.74-7.69 (m, 2H, Ar H), 7.56-7.51 (m, 5H, Ar H), 7.48-7.43 (m, 2H, Ar H); ¹³C{¹H} NMR (400 MHz, CDCl₃): δ 152.11, 149.29, 148.88, 145.64, 138.42, 129.88, 129.74, 128.84, 128.78, 128.70, 128.30, 126.36, 126.11, 125.71, 117.93 ppm.

2 Synthesis of [(TPQ)₃Ir] (1) complex

Synthesis scheme of [(TPQ)₃Ir] (1) complex

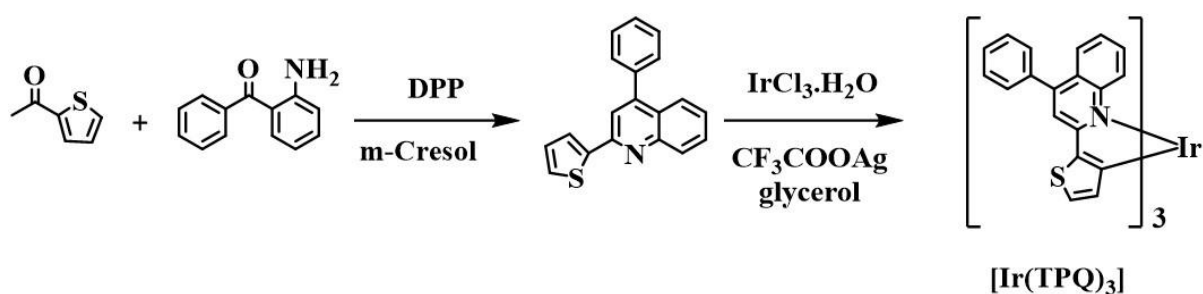


Figure S1: Synthesis of [(TPQ)₃Ir] (1) complex

Characterization of (TPQ)₂Ir₃ (1) complex

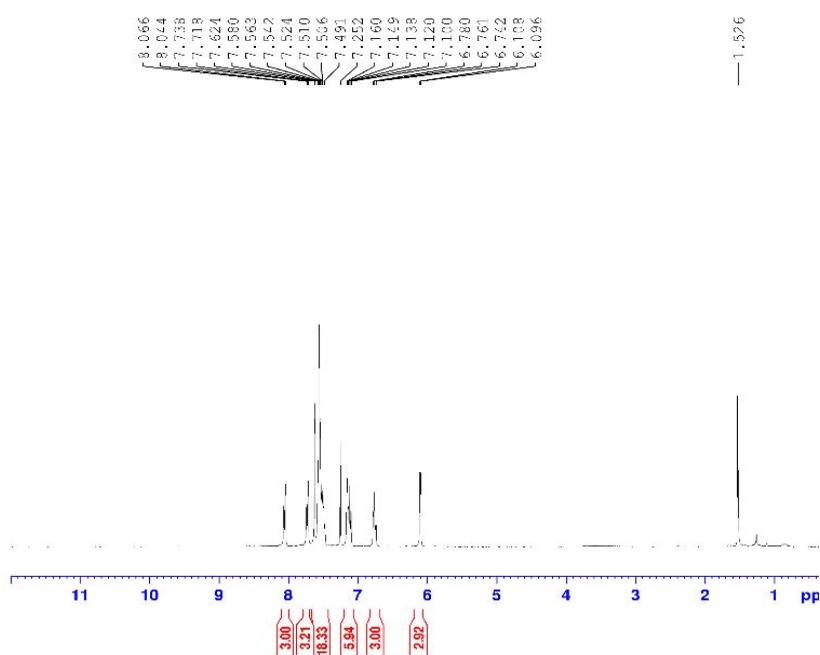


Figure S2: ¹H NMR spectrum of [(TPQ)₃Ir] (1) complex in CDCl₃

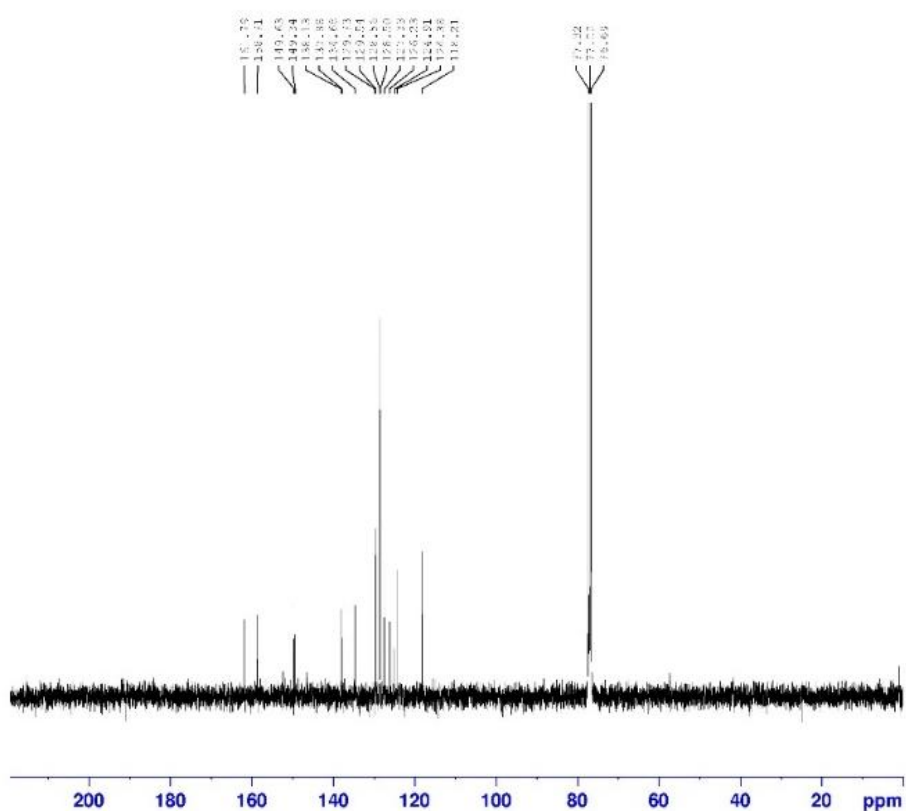


Figure S3: ¹³C{¹H} NMR spectrum of [(TPQ)₃Ir] (1) complex in CDCl₃

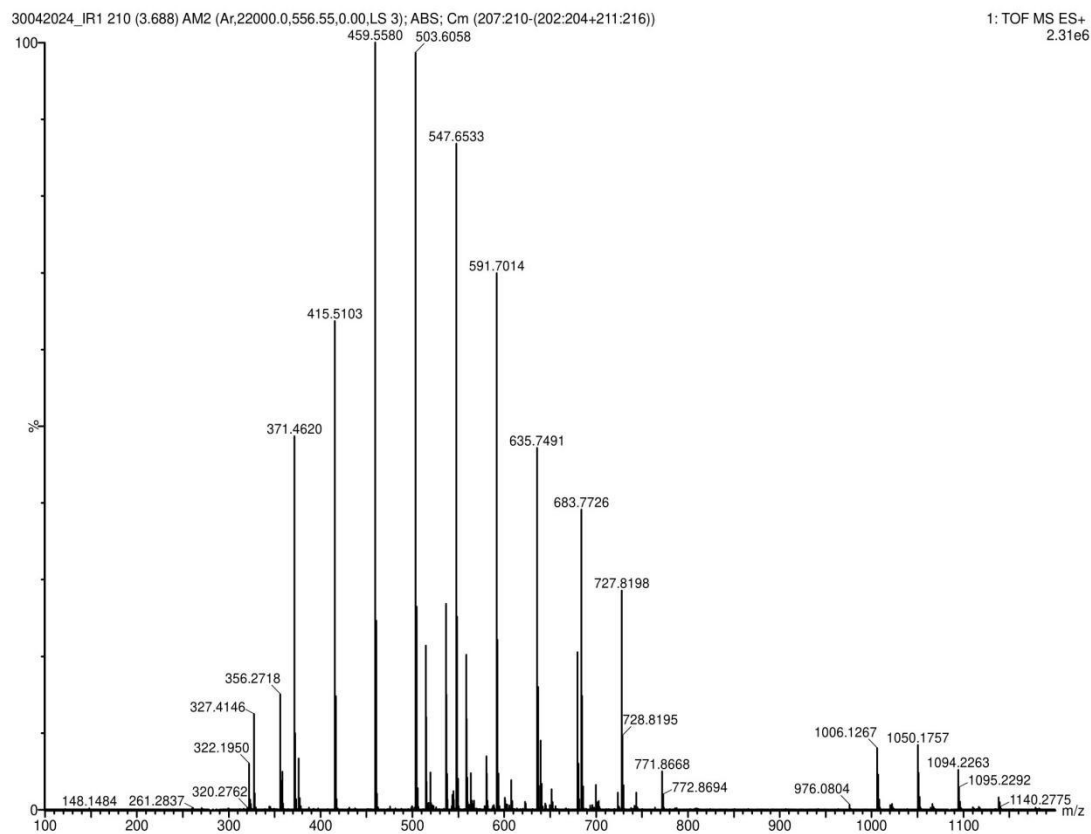


Figure S4: HRMS spectrum of $[(\text{TPQ})_3\text{Ir}]$ (**1**) complex ($[\text{M}+\text{H}]^+$: m/z found 1050.1757; Mol. Wt. 1051.333)

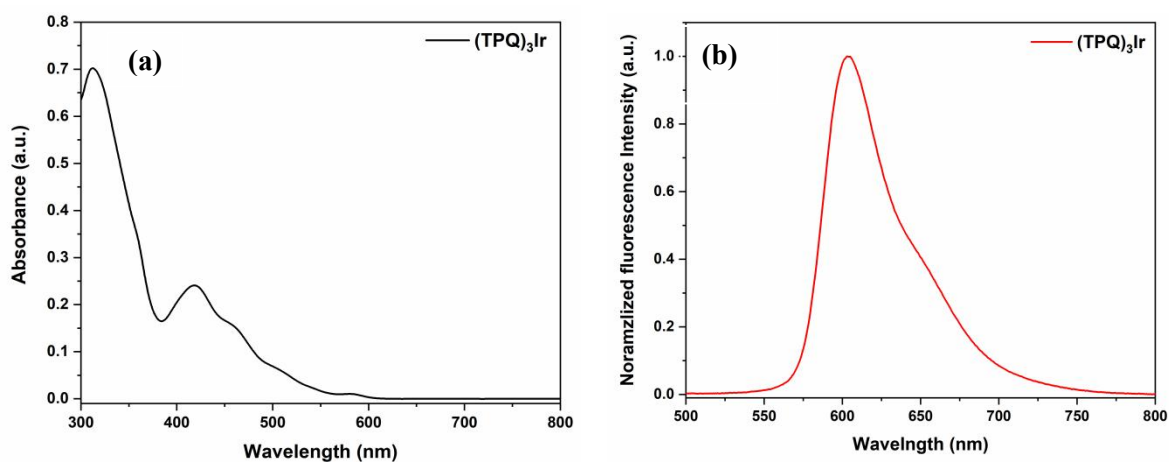


Figure S5: Electronic absorbance and emission spectra of $[(\text{TPQ})_3\text{Ir}]$ (**1**) complex in acetonitrile

3 Synthesis of [(TPQ)₂Ir(4-EO₂-pic)] (2) complex

Synthesis scheme of [(TPQ)₂Ir(4-EO₂-pic)] (2) complex

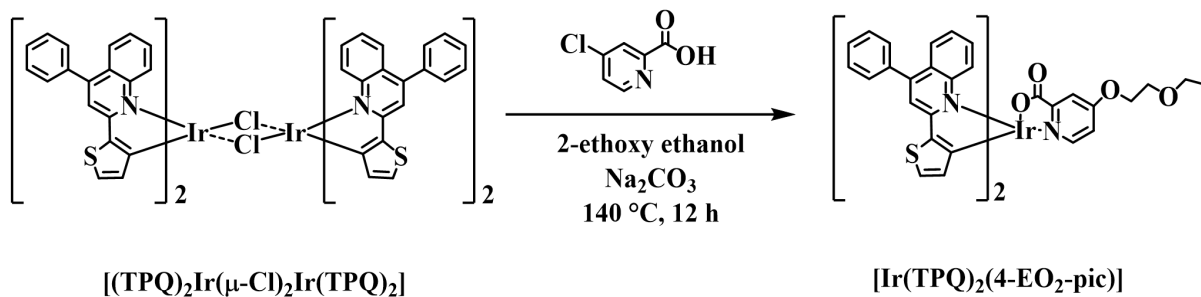


Figure S6: Synthesis of [(TPQ)₂Ir(4-EO₂-pic)] (2) complex

Characterization of [(TPQ)₂Ir(4-EO₂-pic)] (2) complex

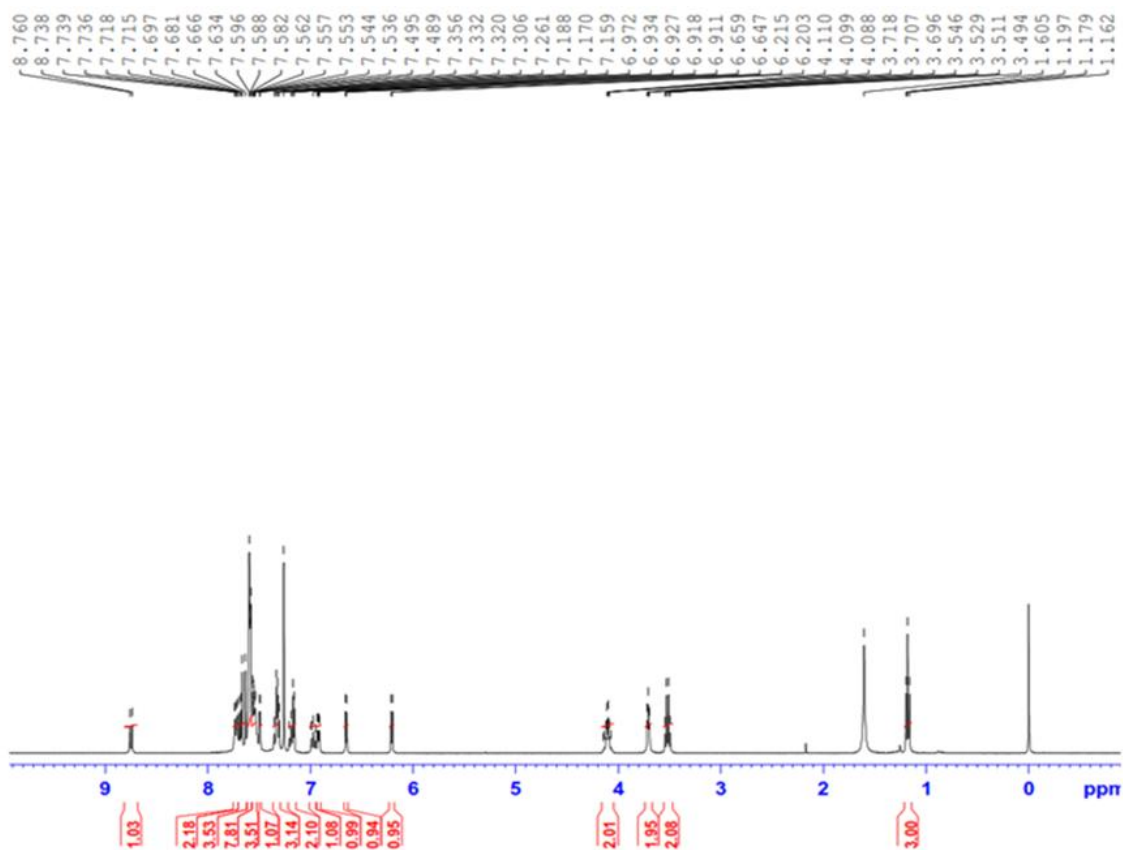


Figure S7: ¹H NMR spectrum of [(TPQ)₂Ir(4-EO₂-pic)] (2) complex in CDCl₃

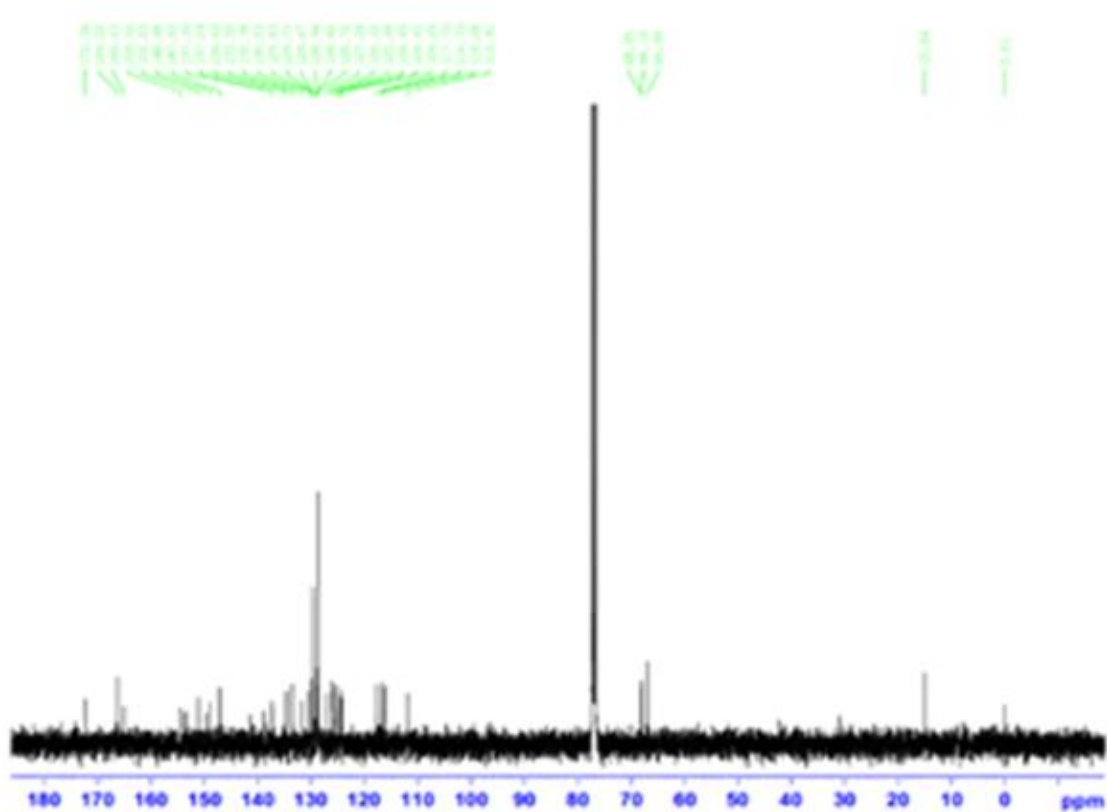


Figure S8: $^{13}\text{C}\{^1\text{H}\}$ NMR spectrum of $[(\text{TPQ})_2\text{Ir}(4\text{-EO}_2\text{-pic})]$ (**2**) complex in CDCl_3

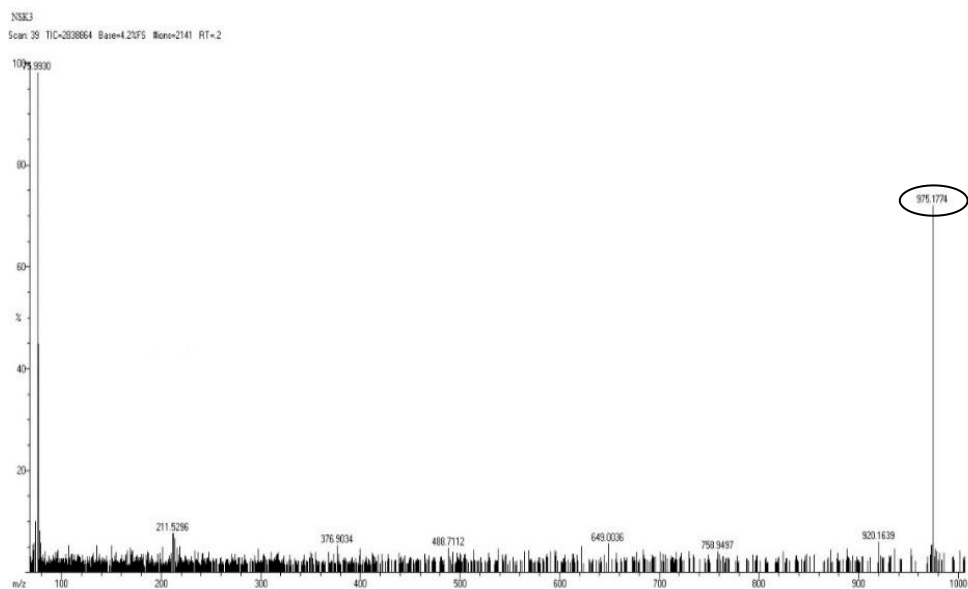


Figure S9: HRMS spectrum of $[(\text{TPQ})_2\text{Ir}(4\text{-EO}_2\text{-pic})]$ (**2**) complex (m/z found 975.1774 $[\text{M}^+]$, Mol. Wt.: 975.1700)

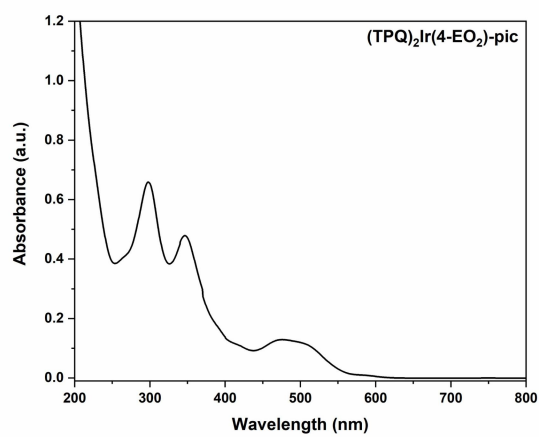


Figure S10: Electronic absorption spectra of $[\text{Ir}(\text{TPQ})_2(4\text{-EO}_2\text{-pic})]$ (**2**) complex in acetonitrile

4 Synthesis of $[(ppy)_2Ir(dfpmPy)]$ (3) complex

Synthesis scheme of $[(ppy)_2Ir(dfpmPy)]$ (3) complex

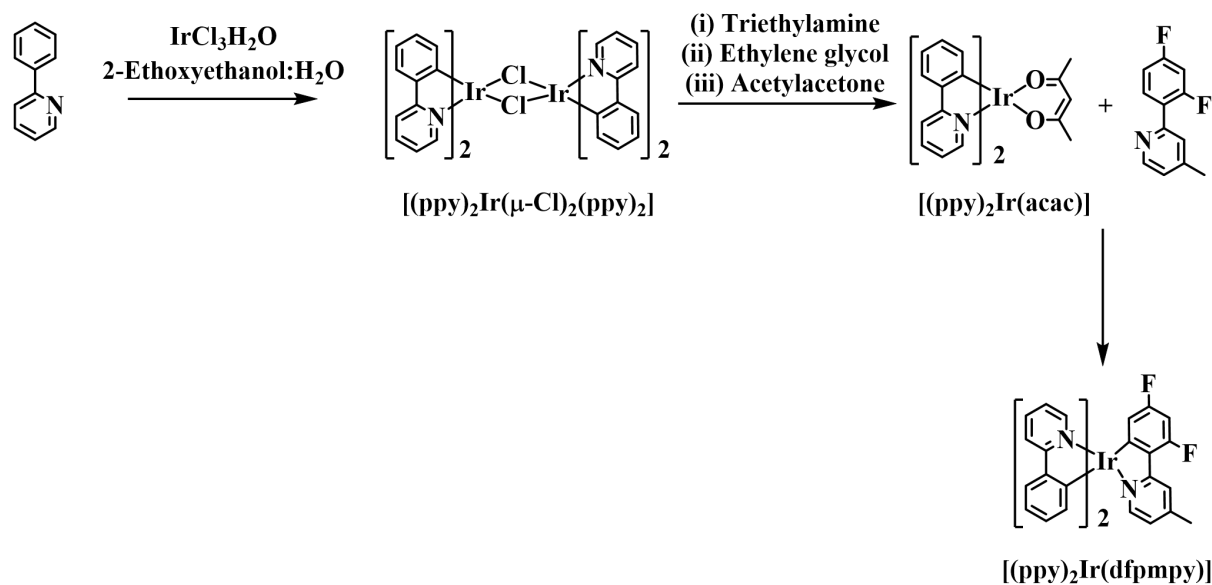


Figure S11: Synthesis of $[(ppy)_2Ir(dfpmPy)]$ (3) complex

Characterization of $[(ppy)_2Ir(dfpmPy)]$ (3) complex

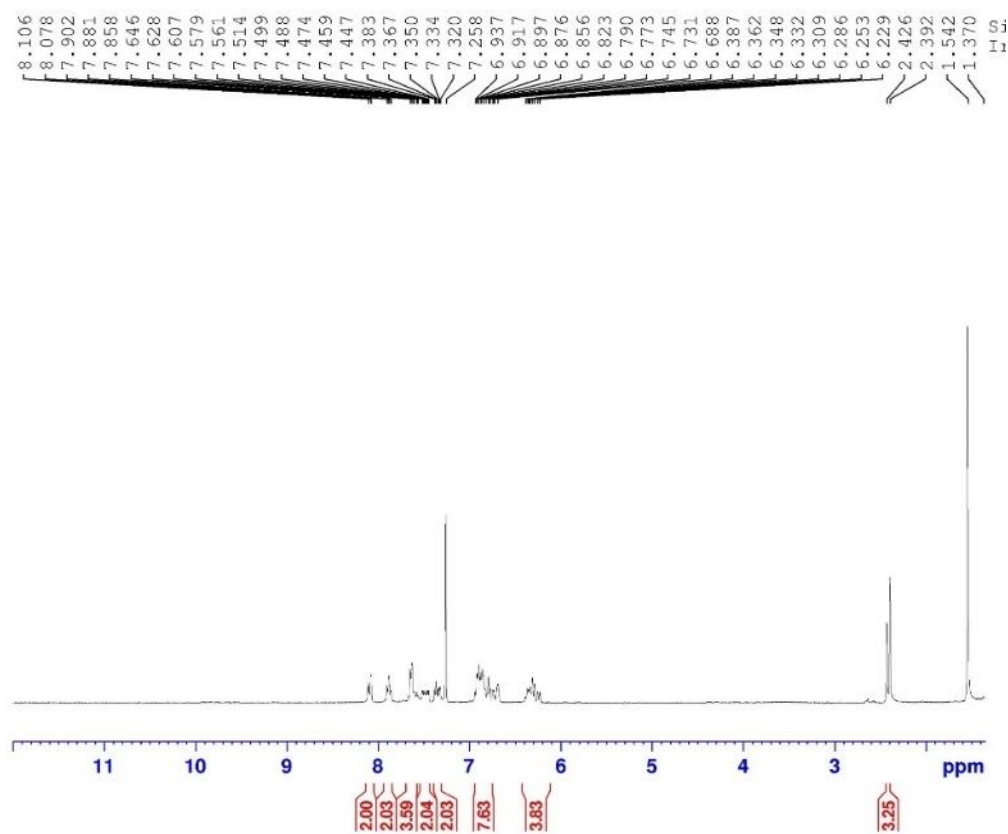


Figure S12: ^1H NMR spectrum of $[(\text{ppy})_2\text{Ir}(\text{dfmpy})]$ (**3**) complex in CDCl_3

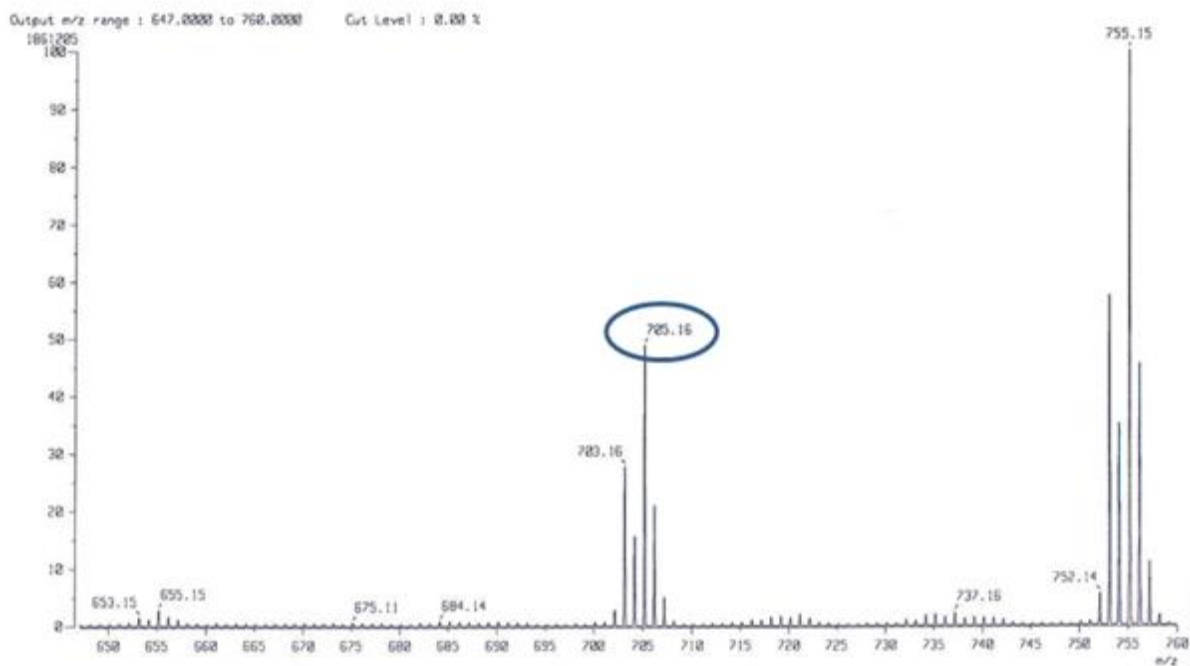


Figure S13: ESI-MS spectrum of $[(\text{ppy})_2\text{Ir}(\text{dfmpy})]$ (**3**) complex $[\text{M} + \text{H}]^+$: m/z found 705.16; Mol Wt: 704.19

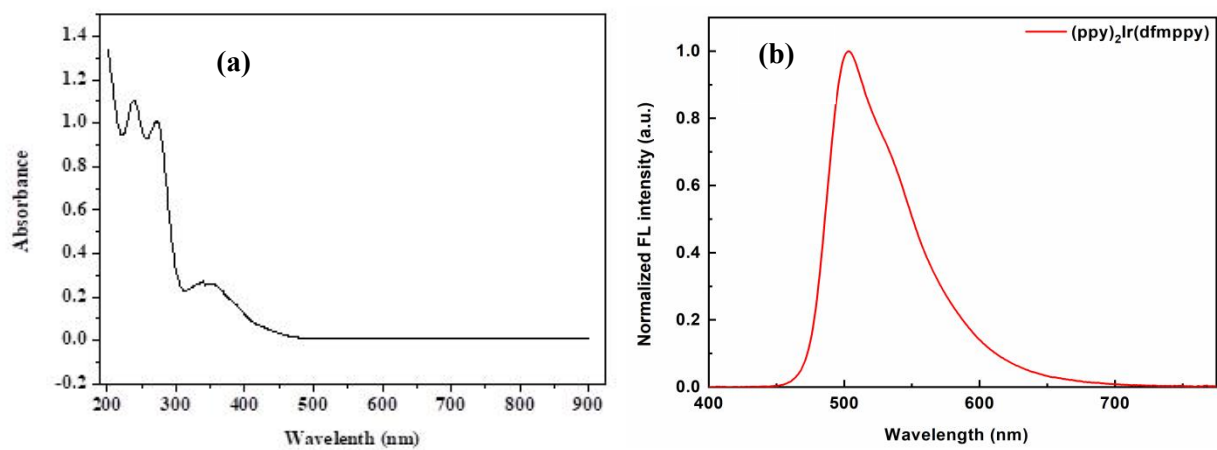


Figure S14: Electronic absorbance and emission spectra of $[(\text{ppy})_2\text{Ir}(\text{dfmpy})]$ (**3**) complex in acetonitrile

5. Flow cytometry overlay histogram

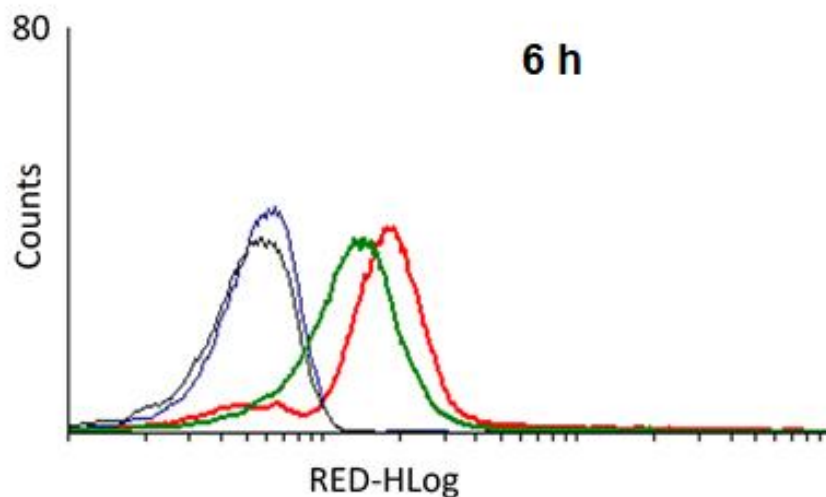


Figure S15: Flow cytometry overlay histogram at 6 h, showing both unstained and compound-treated 4T1 and MDA-MB-231 cells for comparison

In this overlay, black curve represents 4T1 unstained cells, blue curve represents MDA-MB-231 unstained cells, red curve represents compound-treated MDA-MB-231 cells, and green curve represents compound-treated 4T1 cells. The rightward shift observed in the treated populations (red and green) relative to their respective unstained controls (black and blue) indicates cellular uptake of the compound.

While this representative overlay qualitatively demonstrates the difference in uptake between the two cell lines, the quantitative comparison was derived from geometric mean fluorescence intensity (geomean) values obtained from flow cytometry analysis across replicates. These values (17.89 ± 1.31 for MDA-MB-231 and 14.01 ± 0.29 for 4T1) with statistical significance ($p < 0.05$).

6. Bar chart for internalization of $[\text{Ir}(\text{TPQ})_2(4\text{-EO}_2\text{-pic}) (2)$

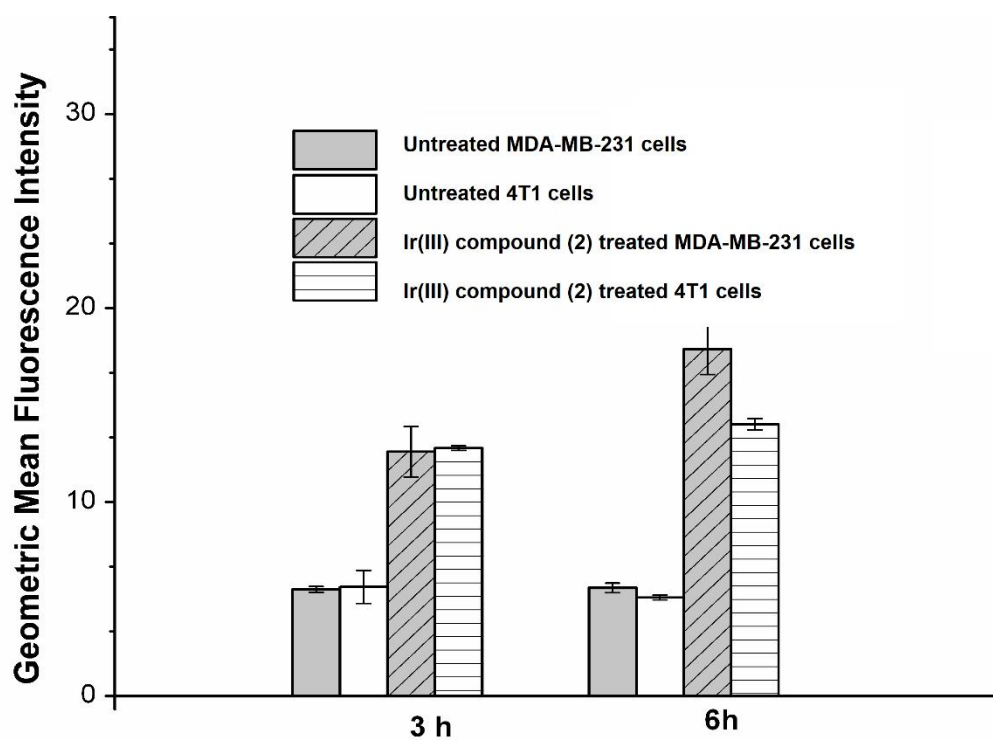


Figure S16: Bar chart correlating with cellular internalization of $[\text{Ir}(\text{TPQ})_2(4\text{-EO}_2\text{-pic}) (2)$